Wind and environmental effects on overhead high voltage transmission lines

A. F. Abdel-Gawad[1, 2] & A.-S. A. Zoklot[2]
[1]*Electrical Power and Machines Engineering Department, Zagazig University, Egypt*
[2]*Mechanical Power Engineering Department, Zagazig University, Egypt*

Abstract

This work is an experimental study of the effect of wind on high voltage transmission lines. Two sets of models, representing a pair of tension towers and a pair of suspension towers, were constructed to a suitable scale. The two sets were tested using a delivery wind tunnel. Three different sizes of conductors were tested at three values of wind speed (5, 10 and 15 m/s). Also, the effect of environmental conditions (ice and mud) was studied. Measurements of the horizontal and vertical displacements of the conductors of different phases were recorded. The additional tension of the conductors, due to aerodynamic drag, was also measured. Useful observations and conclusions are stated.
Keywords: wind effect, transmission lines, high voltage, sag, aerodynamic drag.

1 Introduction

In recent years, as the electric capacity of transmission lines has increased, the size of transmission towers has become larger. Strong wind may cause unexpected damage to the power transmission systems, Fig. 1 [26]. Wind speed and turbulence intensity are greatly affected by terrain and climate, Fig. 2 [25]. In mountainous areas, the terrain effect is manifested in the speed-up of local wind owing to the narrow path caused by the mutual relation of location of mountain ridge and wind direction. Thus, careful study and design are needed when attempting to construct power transmission lines in such wind-hazardous areas. The subject of wind loading on transmission tower-conductor systems was reported in several text books such as [2], [5] and [18]. It is noticed that, in all text books, the wind and ice effects are represented by empirical formulae or

WIT Transactions on Ecology and the Environment, Vol 93, © 2006 WIT Press
www.witpress.com, ISSN 1743-3541 (on-line)
doi:10.2495/SC060411

measurement tables. Generally, these formulae and tables are restricted to certain operating, topographical and meteorological conditions and lack generalization. Gust wind loading and sudden strong winds (typhoons) are not included. Recently, few researchers considered the wind effect on tower-conductor systems. Nakamura *et al.* [13] and Ishikawa *et al.* [6] studied local wind load on transmission tower-conductor systems. The initiative of their work was the unprecedented damage to transmission lines in West Japan that was caused by Typhoon No. 19 in 1991. Their results were based on both wind tunnel measurements and numerical simulations. Similar studies are also available, such as [7-10]. Some projects [16, 22] include the installation of anti-vibrating devices to damp vibrations caused by the conductors exposed to the dynamic load of wind, Fig. 2 [25]. The transmission line conductors may have noncircular cross-sections designed to minimize the effects of wind-induced motions and vibrations [14]. Automatic weather stations may be installed on top of transmission towers to monitor both the mechanical loading of the structures due to wind gusts and the thermal dissipation of conductors for ampacity studies [21]. The environmental effect on the thermal ratings of overhead conductors was investigated by many investigators such as [3, 17, 20, 23]. There are many environmental conditions that have a complicated effect on transmission systems, Fig. 3 [3]. These studies are very helpful in up-rating (increasing the power) transmission lines without violating the thermal limits of the conductors. Also, the effect of ice on transmission lines [24] and ways of de-icing [12] were investigated. Based on the above review, it is obvious that there is a clear shortage in the data of the effects of wind and environmental conditions (ice and mud) on the transmission line systems. This work is a comprehensive parametric study that is based on wind tunnel experimental investigation. The parameters include wind speed, conductor diameter, value of sag, and distribution of ice and mud. Two sets of models that represent a pair of tension towers and a pair of suspension towers were constructed to a suitable scale. The models resemble the 220 kV lattice towers. Measurements of the horizontal and vertical displacements of the conductors of the six phases were recorded. The additional tension of each conductor, due to aerodynamic drag, was measured also. Useful remarks and conclusions are stated.

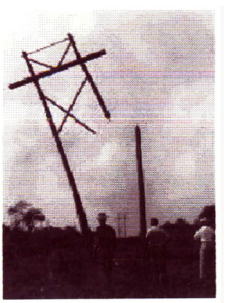

Figure 1: Damage due to strong wind [20].

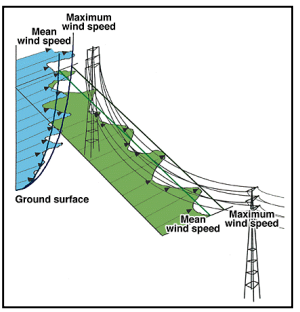

Figure 2: Mean speed and fluctuations of the wind [21].

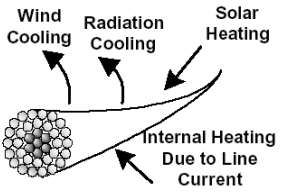

Figure 3: Parameters of the thermal rating [15].

2 Experimental setup

The experiments were performed using an open-circuit atmospheric-exhaust wind tunnel. Room air is pushed through a settling chamber with a honeycomb-type flow straighteners and a 2:1 contraction into a test section of 0.5 × 0.5 m^2. The flow is created by an axial-flow fan that is driven by a 5.5 kW-3 phase motor. At the inlet of the axial fan, a gate is used, as a mechanical method, to control the air speed. The measurements were carried out at three different wind speeds, namely: 5, 10 and 15 m/s. A Pitot-static tube was used to measure the wind speed. The experiments were carried out in the open area that directly follows the exit of the test section of the wind tunnel, Fig. 4.

3 Models and measuring techniques

3.1 Models

Two sets of models that represent a pair of tension towers and a pair of suspension towers were constructed to a scale 1:50. The models resemble the 220 kV lattice, double circuit, single earth wire towers, see Fig. 5. Aluminum and iron rods of L-section were used to construct the models. Rivets and bolts were used to assemble the models. The insulators were replaced by simple suspension arrangements that facilitate the measurement of displacements and additional tension of conductors, Fig. 6. Two wires of diameters 2 and 5 mm were used to resemble the conductors. Another strand conductor of 15 mm-diameter was also investigated. No corrections, to consider the different scaling of towers and conductors, were applied [6].

Figure 4: Experimental setup.

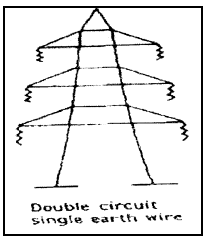

Figure 5: General view of the 220 kV lattice tower.

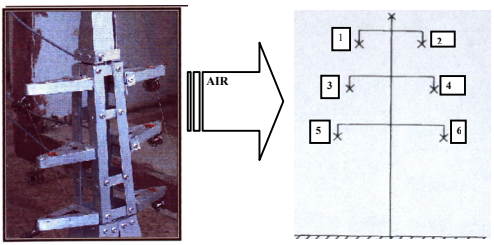

(a) (b)

Figure 6: (a): Close view of the tower suspension; (b): Phase numbering.

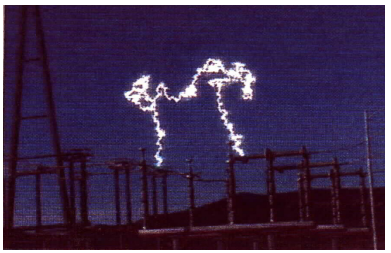

Figure 7: General view of a strong short circuit [20].

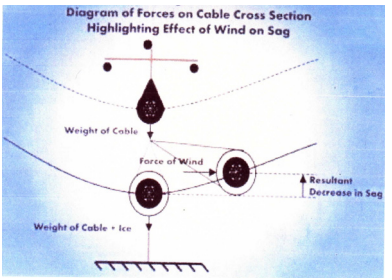

Figure 8: The effect of wind on sag [20].

3.2 Measurement of horizontal and vertical displacements

The horizontal displacement of the conductor changes the safe distance between conductors. In severe wind conditions, when conductors approach each other, a strong short circuit may be expected, Fig. 7 [26]. This situation may be demonstrated by Warrington's formula [18] as follows:

$$\text{Still air: } R_{arc} = 8750\, L_{sc} / I^{1.4} \tag{1}$$

$$\text{Cross wind blowing: } R_{arc} = 8750\, (S_c + 3\, V_a\, t) / I^{1.4} \tag{2}$$

where L_{sc} is the length of arc (ft) in still air and equals to the conductor spacing, I is fault current (amps.), S_c is the conductor spacing (ft), V_a is the wind speed (mph), and t is the arc duration (Sec.). Thus, a strong damage may occur to the transmission-line system. On the other hand, the vertical displacement of the conductor changes its natural (or preset) sag, Fig. 8 [26]. In still air, tension-sag relation takes the form:

$$T = \frac{\rho_L\, g\, L^2}{8\, S} \tag{3}$$

where T is the mechanical tension in the conductor, ρ_L is the mass of conductor per unit length, L is the span of the conductor, g is the gravitational acceleration, and S is the sag at the mid-point of the span. Continuous blowing of wind may reduce sag and increase the clearance between the conductor and earth. Traditional means of measuring the distance are not practical in the present case where changes of the position of the mid-point of the span in the vertical and horizontal directions are to be measured. The traditional means interfere with the air that exits from the wind tunnel. This may change the air speed, direction, and quality. Two laser pointers were used simultaneously to measure the horizontal (ΔX) and vertical (ΔY) displacements. The laser pointers are forced to slide in the horizontal and vertical directions on a simple steel frame. Before turn-on of the wind tunnel (V_a = 0.0), the two pointers are moved until their lights intersect with the mid-point of the span of conductor. Thus, the initial horizontal (X_o) and vertical (Y_o) coordinates are determined. Then, while the air is blowing at certain speed, the horizontal and vertical pointers are moved so that their lights intersect again with the mid-point of the span of conductor. Thus, the final horizontal (X_f)

and vertical (Y_f) coordinates are determined. So, the displacements due to wind are found from:

$$\text{Normalized horizontal displacement:} \quad \Delta X_n = (X_f - X_o)/L \tag{4}$$

$$\text{Normalized vertical displacement:} \quad \Delta Y_n = (Y_f - Y_o)/L \tag{5}$$

3.3 Measurement of additional tension

A simple force balance was used to measure the additional tension of the conductor of each phase due to wind, Fig. 4. The force balance is consisted of a small water container, which is scaled to give the volume of water, a pair of small pulleys and a wire that connects one end of the conductor to the water container over the pulleys. Before turn-on of the wind tunnel (V_a = 0.0), the mid-point of the span of the conductor is adjusted to the required sag by adding a volume of water (Q_o) to the container. The vertical position of the container is determined. When the air blows at certain speed (V_a), the conductor is pushed to move and consequently the container moves upwards. Water is added again to restore the initial position of the container. The final volume of water is Q_f. The additional force due to wind is found from:

$$T_w = (Q_f - Q_o)\,\rho_w\, g \tag{6}$$

where ρ_w is the water density and g is the gravitational acceleration. All measurements were carried out at steady values of the air velocity. The effect of wind fluctuations can be evaluated by considering the gust effect factor (GEF) [7-10]. The equivalent wind loading is equal to the mean wind force multiplied by a GEF. The GEF accounts for the dynamics of wind fluctuations and the load amplification introduced by the transmission-system dynamics. Values of GEF are found in the international codes and standards of wind loading according to the operating conditions.

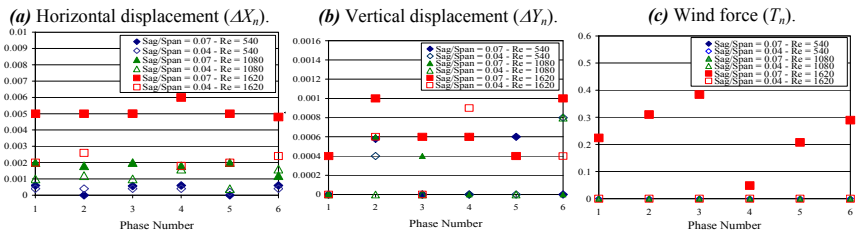

Figure 9: Variation of ΔX_n, ΔY_n and T_n - tension towers, $d_{conductor}$ = 2 mm.

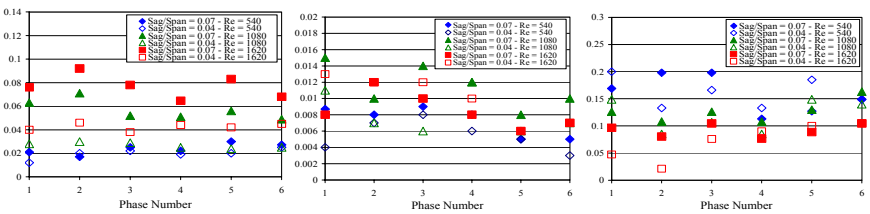

Figure 10: Variation of ΔX_n, ΔY_n and T_n - suspension towers, $d_{conductor}$ = 2 mm.

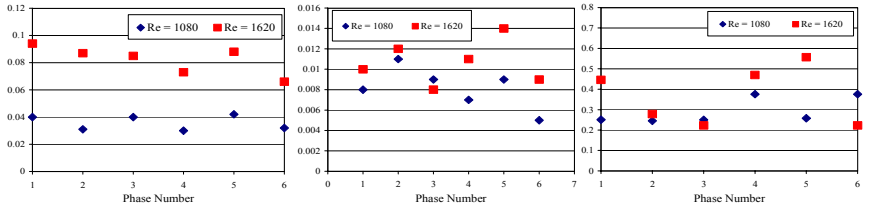

Figure 11: Variation of ΔX_n, ΔY_n and T_n - suspension towers - with distributed mud, $d_{conductor}$ = 2 mm.

4 Results and discussions

4.1 Experimental measurements

Three wind speeds (5, 10 and 15 m/s) were applied in the experiments. Three conductor diameters (2, 5 and 15 mm) were used in the investigation. Figures 9-11 show the variation of horizontal and vertical displacements as well as additional tension for a conductor diameter of 2 mm. From Fig. 9, for the tension towers, it is clear that the normalized horizontal displacement (ΔX_n) increases with both sag and wind velocity. The normalized vertical displacement (ΔY_n) changes by small amounts with wind speed. For the smaller sag (sag/span = 0.04) almost no change is noticed for Re = 540 and 1080 (Re is the Reynolds number = $\rho_a V_a d/\mu_a$). The normalized wind force (T_n) is obtained by dividing the additional wind force (Eq. 6) by the original conductor tension ($T = \rho_w g Q_o$). No additional force is recorded expect for Re = 1620 and sag/span = 0.06 where $T_w \cong$ 25 % T. From Fig. 10, for the suspension towers, it is noticed that ΔX_n and ΔY_n increase with both sag and wind speed. However, T_n decreases slightly with the wind speed. It seems that conductors are free to move with the increase of wind speed without much increase of T_n. Comparing Figs. 9 and 10, it is obvious that values of ΔX_n, ΔY_n and T_n for the suspension towers are one order of magnitude higher than those of the tension towers. To consider the effect of mud, three pieces of mud were distributed equally along each conductor. The effect of mud on ΔX_n, ΔY_n and T_n is shown in Fig. 11. Comparing Figs. 10 and 11, it is clear that mud has a small effect on both ΔX_n and ΔY_n. However, the values of $[T_n]_{mud}$ are 2 to 4 times the values of T_n without mud. This may be attributed partially to the increase of overall weight of the conductor but mainly to the additional disturbance created by mud pieces in the flow field around the conductors. These conductors take the form of circular cylinders with coshine distribution. Thus, a big increase of the aerodynamic drag is expected. Figures 12 and 13 illustrate the variations of ΔX_n, ΔY_n and T_n for different values of sag/span and wind speed at a conductor diameter of 5 mm. It is demonstrated that the values of ΔX_n and ΔY_n of the suspension towers are one-order of magnitude higher than the tension towers. Values of $[T_n]_{suspension}$ equals 4-6 $[T_n]_{tension}$. Comparing Figs. 10 and 13, it is found that $[T_n]_{d=5\ mm} \cong$ 3-4 $[T_n]_{d=2\ mm}$. Figures 14 and 15 show the variations of

ΔX_n, ΔY_n and T_n for a strand conductor of d = 15 mm. The effect of distributed mud or complete mud on the conductor is shown in Fig. 14. The case of complete mud resembles the case of ice covering the whole conductor with increase of 3 mm in diameter. Almost the same range of ΔX_n and ΔY_n is obtained for both complete and distributed mud cases. For Re = 12150, $[T_n]_{distributed\ mud}$ is relatively greater than $[T_n]_{complete\ mud}$. Comparing Figs. 10, 13 and 15, it is obvious that the increase of the diameter of the conductor increases considerably the values of ΔX_n, ΔY_n and T_n. This may be attributed to the change of the wake pattern behind the conductor [4, 15]. Thus, the aerodynamic drag increases with diameter (which means the increase of Reynolds number) and thus pushes the conductor horizontally and vertically. An important point to state is that there is a noticeable mutual aerodynamic interference between the conductors of different phases. However, this point needs deeper investigation [1, 11, 19]. Also, deeper knowledge is needed on the swinging and clashing risks of cables in large bundles without spacers.

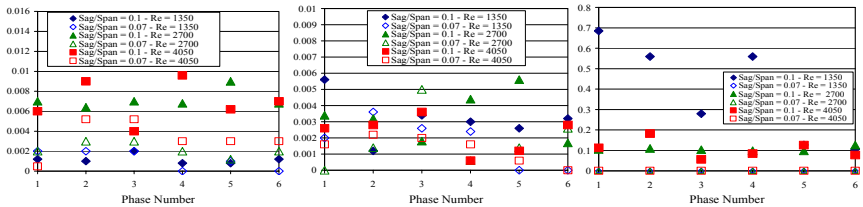

Figure 12: Variation of ΔX_n, ΔY_n and T_n - tension towers, $d_{conductor}$ = 5 mm.

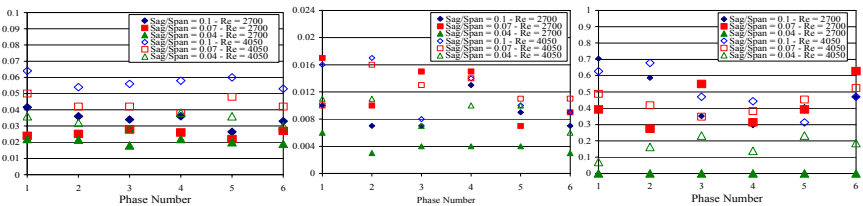

Figure 13: Variation of ΔX_n, ΔY_n and T_n - suspension towers, $d_{conductor}$ = 5 mm.

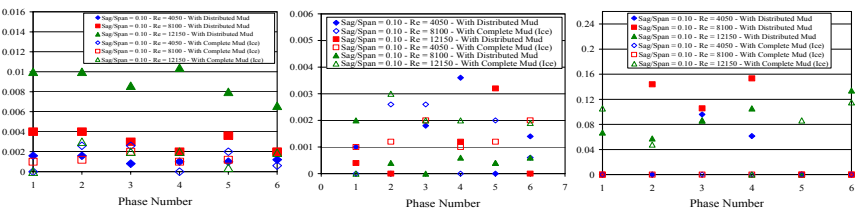

Figure 14: Variation of ΔX_n, ΔY_n and T_n - tension towers - strand conductor, $d_{conductor}$ = 15 mm.

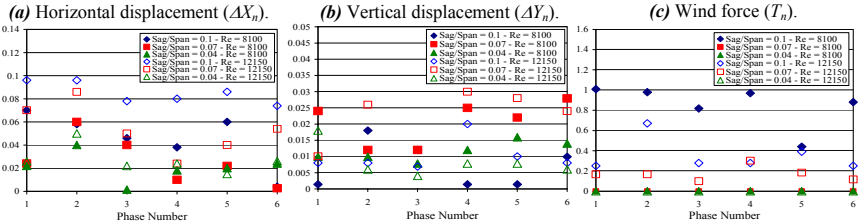

Figure 15: Variation of ΔX_n, ΔY_n and T_n - suspension towers - strand conductor, $d_{conductor}$ = 15 mm.

4.2 Least-squares regression

In order to generalize the measurements, least-squares regression was used to find the relation between the different parameters that affect the normalized vertical and horizontal displacements as well as normalized additional wind load. Two types of curve regression were applied, namely: multiple linear and multiple exponential. They take the following forms:

1-Multiple Linear:

$$\text{(i) } \Delta X_n = a_{ox} + a_{1x}\,(Ph) + a_{2x}\,Re + a_{3x}\,\rho_{Ln} + a_{4x}\,S_n \quad (7)$$

$$\text{(ii) } \Delta Y_n = a_{oy} + a_{1y}\,(Ph) + a_{2y}\,Re + a_{3y}\,\rho_{Ln} + a_{4y}\,S_n \quad (8)$$

$$\text{(iii) } T_n = a_{ot} + a_{1t}\,(Ph) + a_{2t}\,Re + a_{3t}\,\rho_{Ln} + a_{4t}\,S_n \quad (9)$$

2-Multiple Exponential:

$$\text{(i) } \Delta X_n = a_{ox}\,exp[\,a_{1x}\,(Ph) + a_{2x}\,Re + a_{3x}\,\rho_{Ln} + a_{4x}\,S_n] \quad (10)$$

$$\text{(ii) } \Delta Y_n = a_{oy}\,exp[\,a_{1y}\,(Ph) + a_{2y}\,Re + a_{3y}\,\rho_{Ln} + a_{4y}\,S_n] \quad (11)$$

$$\text{(iii) } T_n = a_{ot}\,exp[\,a_{1t}\,(Ph) + a_{2t}\,Re + a_{3t}\,\rho_{Ln} + a_{4t}\,S_n] \quad (12)$$

Table 1: The regression coefficients for the suspension towers.

Coefficient / Regression	a_{ox}	a_{1x}	a_{2x}	a_{3x}	a_{4x}	a_{oy}	a_{1y}	a_{2y}	a_{3y}	a_{4y}	a_{ot}	a_{1t}	a_{2t}	a_{3t}	a_{4t}
Linear	2 $\times10^{-2}$	- 215 $\times10^{-5}$	818 $\times10^{-8}$	- 48 $\times10^{-2}$	54 $\times10^{-2}$	655 $\times10^{-5}$	224 $\times10^{-6}$	727 $\times10^{-9}$	- 24 $\times10^{-3}$	4 $\times10^{-2}$	- 236 $\times10^{-3}$	- 62 $\times10^{-4}$	313 $\times10^{-7}$	1624 $\times10^{-3}$	736 $\times10^{-2}$
Exponential	102 $\times10^{-2}$	- 215 $\times10^{-5}$	818 $\times10^{-8}$	- 48 $\times10^{-2}$	54 $\times10^{-2}$	100657 $\times10^{-5}$	224 $\times10^{-6}$	727 $\times10^{-9}$	- 24 $\times10^{-3}$	4 $\times10^{-2}$	79 $\times10^{-2}$	- 62 $\times10^{-4}$	313 $\times10^{-7}$	1624 $\times10^{-3}$	736 $\times10^{-2}$

Table 2: The regression coefficients for the tension towers.

Coefficient / Regression	a_{ox}	a_{1x}	a_{2x}	a_{3x}	a_{4x}	a_{oy}	a_{1y}	a_{2y}	a_{3y}	a_{4y}	a_{ot}	a_{1t}	a_{2t}	a_{3t}	a_{4t}
Linear	- 24 $\times10^{-4}$	- 4 $\times10^{-5}$	17 $\times10^{-7}$	- 5 $\times10^{-2}$	7 $\times10^{-2}$	11 $\times10^{-4}$	- 71 $\times10^{-6}$	- 17 $\times10^{-8}$	25 $\times10^{-3}$	285 $\times10^{-4}$	-136 $\times10^{-3}$	- 11 $\times10^{-3}$	- 29 $\times10^{-6}$	- 54 $\times10^{-2}$	468 $\times10^{-2}$
Exponential	998 $\times10^{-3}$	- 4 $\times10^{-5}$	17 $\times10^{-7}$	- 5 $\times10^{-2}$	7 $\times10^{-2}$	999 $\times10^{-3}$	- 71 $\times10^{-6}$	- 17 $\times10^{-8}$	25 $\times10^{-3}$	285 $\times10^{-4}$	873 $\times10^{-3}$	- 11 $\times10^{-3}$	- 29 $\times10^{-6}$	- 54 $\times10^{-2}$	468 $\times10^{-2}$

Matlab 6.1 package was used to find the coefficients of Eqs. 7-12. Tables 1 and 2 show the coefficients for both the linear and exponential regression for the suspension and tension towers, respectively. Figs. 16 and 17 show the results of regression for some test cases. It is clear that linear regression gives the best

results. When considering the values of a_1, it is obvious that the phase location has a smaller effect on ΔX_n, ΔY_n and T_n than other factors except Re. The values of the coefficient a_2 show that, within the tested values of Reynolds number, Re has almost negligible effect on ΔX_n, ΔY_n and T_n.

A summary of a general scheme (methodology) of the effect of wind/environment conditions on the power transmission lines is shown in Fig. 18. The scheme covers other aspects than those considered in the present study.

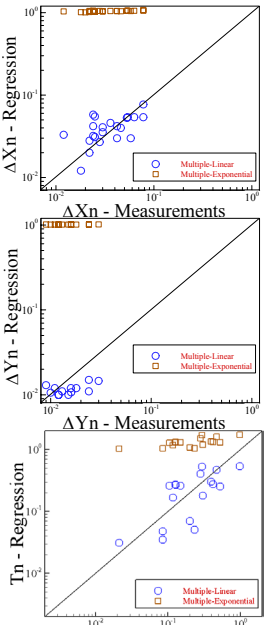

Figure 16: Regression results for the suspension towers.

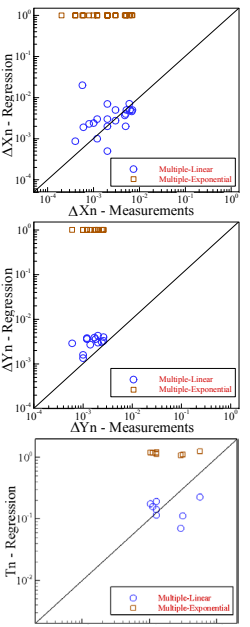

Figure 17: Regression results for the tension towers.

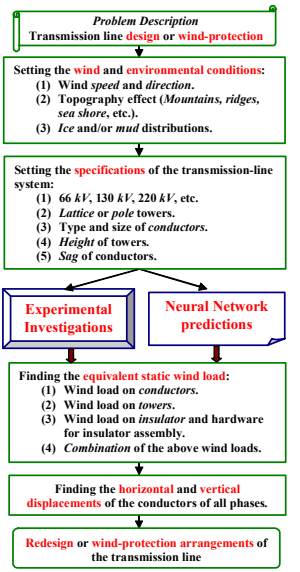

Figure 18: General scheme of the wind-effect study.

5 Conclusions

The present study is an experimental investigation of the effect of environmental conditions on high voltage transmission lines. Different parameters were investigated such as conductor diameter and phase, wind speed, tower type, and distribution of mud. The horizontal and vertical displacements as well as the additional tension, due to wind, of the conductors are recorded. From the above discussions, the following points can be stated:

1. Generally, the values of ΔX_n, ΔY_n and T_n depend on conductor diameter, wind speed, sag and distribution of mud.

2. For tension towers, the wind effect on ΔX_n, ΔY_n and T_n appears mainly at the highest value of speed (V_a = 15 *m/s*).
3. Generally, for suspension towers, values of ΔX_n, ΔY_n and T_n may reach one-order of magnitude higher than those of tension towers.
4. Distributed mud has a small effect on both ΔX_n and ΔY_n. However, distributed mud increases the values of T_n by 2-4 times the values without mud.
5. Increasing the conductor diameter increases considerably the values of ΔX_n, ΔY_n and T_n.
6. For suspension towers, T_n may reach 40-50%. Whereas, for tension towers, T_n may reach 10-25%.
7. Increasing the values of ΔX_n, ΔY_n and T_n may be attributed to the change of the wake pattern behind the conductor. Thus, the aerodynamic drag pushes the conductor horizontally and vertically.
8. There is a mutual aerodynamic interference between the different phases that need deeper investigation.
9. Further investigations are needed to estimate wind load on tower structure.

The authors wish that the present investigation contributes to wide the spectrum of understanding the wind effect on high voltage transmission systems, simplify the wind load evaluation method, and improve the design tools. The authors also believe that further investigations are certainly needed.

References

[1] Ahmed, A. & Ostowari, C., Longitudinally and transversely spaced cylinders in cross flow. *Wind Eng. Ind. Aerodyn.*, **36**, pp. 1095-1104, 1990.

[2] Bayliss, C., *Transmission and Distribution Electrical Engineering*, 2nd-Edition, Newnes-Elsevier Publisher, 1999.

[3] Daconti, J. R., *Increasing power transfer capability of existing transmission lines*, Power Technologies, Inc., 2003, http://www.ewh.ieee.org/r1/schenectady/feb21_2003_lecture.pdf.

[4] Fujisawa, N. & Nakabayashi, T., Neural network control of vortex shedding from a circular cylinder using rotational feedback oscillations. *Fluids & Structures*, **16 (1)**, pp. 113-119, 2002.

[5] Grigsby, L. L., *The Electric Power Engineering Handbook*, CRC Press-IEEE Press, 2001.

[6] Ishikawa, T., *et al.*, *Establishment of recommendations for wind loads on transmission towers – a draft*, http://criepi.denken.or.jp/en/e_publication/a2003/03seika38.pdf.

[7] Ishikawa, T. & Nakamura, H., Derivation of gust response factor for transmission steel tower. *Abiko Research Laboratory Rep. No. U97100*, CRIEPI, 1998.

[8] Ishikawa, T. & Nakamura, H., Derivation of gust response factor and maximum horizontal tension of aerial cables. *Abiko Research Laboratory Rep. No. U98004*, CRIEPI, 1998.

[9] Ishikawa, T., Study on wind load evaluation method considering the dynamic effect for transmission towers. *Structural Mechanics and Earthquake Eng.*, JSCE, **738**, **I-64**, 2003.
[10] Ishikawa, T., *et al.*, Evaluation techniques of wind load and gust response for overhead transmission lines. *CRIEPI review*, **48**, 2003.
[11] Matsumoto, M., Shiraishi, N. & Shirato, H., Aerodynamic instabilities of twin circular cylinders. *Wind Eng. Ind. Aerodyn.*, **33**, pp. 91-100, 1990.
[12] McCurdy, J. D., Sullivan, C. R. & Petrenko, V. F., Using dielectric losses to de-ice power transmission lines with 100 kHz high-voltage excitation, *IAS* 2001, http://thayer.dartmouth.edu/other/inductor/papers/hfdeice.pdf.
[13] Nakamura, H., *et al.*, *Studies on local wind and wind-resistance design of transmission tower-conductor systems*, http://criepi.denken.or.jp/en/e_publication/a1999/99seika26.pdf.
[14] Peterson Jr., A. J. & Hoffmann, S., *Transmission line conductor design comes of age*, 2003, http://www.findarticles.com/articles/mi_m0CXO/is_6_55/ai_103697698.
[15] Prasad, A. & Williamson, C. H. K., A method for the reduction of bluff body drag. *Wind Eng. Ind. Aerodyn.*, **69-71**, pp. 155-167, 1997.
[16] Putnam, E., *Country negotiates power line deal*, Wausau Daily Herald, 2004, http://www.wausaudailyherald.com/wdhlocal/294057820857405.shtml.
[17] Raniga, J. & Rayudu, R. K., Stretching transmission line capabilities – A transpower investigation, Institution of Professional Engineers, New Zealand, http://www.cfacs.co.nz/download/Dlripenz.pdf.
[18] Ryan, H. M., *High Voltage Engineering and Testing*, 2nd-Edition, IEE, 2001.
[19] Tokoro, S., Komatsu, H., Nakasu, M., Mizuguchi, K. & Kasuga, A., A study on wake-galloping employing full aeroelastic twin cable model. *Wind Eng. Ind. Aerodyn.*, **88**, pp. 247-261, 2000.
[20] For Uprating Overhead Lines, Shaw Power Technologies, Inc., 2004, www.shawgrp.com/PTI/consulting/transmission/rating_monitor.cfm.
[21] Monitoring Transmission Lines, VAISALA, Finland, www.vaisala.com/DynaGen_Attachments/Att33124/VN165_p19.pdf.
[22] National Power Transmission Co. "Transelectrica" SA, Romania, Project No. 33354, 2004, http://www.ebrd.com/projects/psd/psd2004/33354.htm.
[23] Upgrading Transmission Capacity for Wholesale Electric Power Trade, www.eia.doe.gov/cneaf/pubs_html_feat_trans_capacity/w_sale.html.
[24] Winter Storms, http://www.ci.eugene.or.us/HRRS/EmerPlan/MHMPch7WinterStrms.pdf.
[25] http://criepi.denken.or.jp.
[26] Free download from Internet.